NeuroImage 150 (2017) 112–118

Contents lists available at ScienceDirect

NeuroImage

journal homepage: www.elsevier.com/locate/neuroimage

Activity and connectivity of the cerebellum in trigeminal nociception

Jan Mehnert[a], Laura Schulte[a], Dagmar Timmann[b], Arne May[a,*]

[a] Department of Systems Neuroscience, University Medical Center Eppendorf, Hamburg, Germany
[b] Department of Neurology, University of Duisburg-Essen, Germany

ARTICLE INFO

Keywords:
Cerebellum
Brainstem
Pain
Migraine
Trigeminal nociception
Functional connectivity
Modulation of pain intensity

ABSTRACT

The role of the cerebellum in pathologies of the trigeminal nervous system is still unknown although recently gathered evidence point to a modulatory rather than a passive role. Here we provide evidence for the activation of specific cerebellar areas during nociceptive trigeminal input in the left nostril in a large number of volunteers (54 subjects) and an additional independent group (18 subjects) as measured by functional magnetic resonance imaging (fMRI). Peak voxel activity ipsilateral to the stimulated side can be seen in cerebellar lobules VI, VIIIa and Crus I, and vermal lobule VIIIa, although some activations are also seen in the contralateral side. The individuals' intensity and unpleasantness ratings are mostly processed in the hemispheric lobules VI stretching to V, representing the face areas of the cerebellar's fractured homunculus. We found a robust functional connectivity during nociception between the cerebellum and the rostral part of the pons as well as the periaqueductal grey and the thalamus, involving the descending antinociceptive network as well as areas known to form close loops with the cerebellum in the motor domain. Cerebellar connectivity with higher cortical areas include most of the known hubs in pain processing which are the insular cortex, operculum and putamen, and the face areas in the precentral gyrus. The current data provide a solid basis for further research of the cerebellar's activity and connectivity in primary headache and facial pain syndromes.

Introduction

The functional influence of the cerebellum on pain processing is unknown (Saab and Willis, 2003) but gathers increased interest. In a recent metaanalysis Moulton and colleagues showed that multiple cerebellar areas are commonly activated during nociceptive processing in humans (Moulton et al., 2010) and that some of these areas partly overlap with areas processing other aversive sensory input (Moulton et al., 2011). In 2003 it was demonstrated that the cerebellum might compute intensity rating to thermal painful stimuli (Helmchen et al., 2003). Deeper evidence stems from the study of Ruscheweyh and colleagues (Ruscheweyh et al., 2014), which causally linked cerebellar circumscribed damage due to infarction to more sensitivity for painful stimuli, but also deficient inhibition in response to placebo and offset analgesia. This indicates that the cerebellum holds not just a passive role in pain transmission, or possibly just motor reaction to nociceptive input, but plays an important, yet underestimated, role in pain transmission and even pain perception and control.

Although there is ample evidence that the cerebellum might play a significant role in trigeminal nociceptive pain, such a migraine, surprisingly little research went into disentangling this function. Most functional imaging studies show cerebellar activity in migraine and other headache syndromes (May, 2009, 2013), however these findings are at best reported but not discussed (May, 2009, 2013). Anatomically, the functional involvement of the cerebellum in migraine is supported by direct connection with the spinal trigeminal nucleus in cats (Carpenter and Hanna, 1961) and rats (Huerta et al., 1983). Nevertheless, little is known about functional consequences or even which specific areas of the cerebellum are involved in trigeminal nociception. The two fractured representations of the homunculus in the anterior and posterior part of the cerebellars' hemispheres (Manni and Petrosini, 2004) are candidates, where trigemino-cerebellar projections should terminate in the represented face areas, while a third representation of the homunculus in the cerebellums vermis is under discussion (Rijntjes et al., 1999) and, thereby, serves as a further candidate of trigeminal nociceptive processing. Furthermore, also other lobules might play an important role such as the posterolateral hemisphere (Crus I, Crus II), where the processing of cognition is presumed (Stoodley and Schmahmann, 2011; Timmann et al., 2010), and where pain might be rated cognitively.

Focusing on the cerebellar role in trigeminal pain processing, we used functional magnetic resonance imaging (fMRI) in a large number of healthy subjects during chemosensory nociceptive stimulation of the left nostril to gain a deeper understanding of the cerebellar's activity,

* Corresponding author.
E-mail address: a.may@uke.de (A. May).

http://dx.doi.org/10.1016/j.neuroimage.2017.02.023
Received 23 November 2016; Accepted 9 February 2017
Available online 10 February 2017
1053-8119/

modulation and connectivity in trigeminal pain. We verified our findings using an independent control group.

Methods

Subjects and experimental design

Fifty-four healthy volunteers (mean age: 26.0 ± 3.9; 31 females) participated in an experiment on trigeminal nociception following the protocol of Stankewitz et al. (2010). The experiment consists of four conditions, namely 1) the transmission of gaseous ammonia (concentration of 2.5%), which induces a painful, trigeminal sensation, 2) the transmission of rose odor and 3) simple air puffs mixed in an constant dry air flow (74.4 ml/s) into the left nostril, while they were breathing through their mouth top prevent sniffing and movements using an olfactometer. The duration of the stimulations was set to 0.8 s. A further repetitive visual stimulation using a rotating circle with checkerboard-like pattern at 8 Hz (duration of 4 s) served as a visual control condition but was not further analyzed in the current study. During the experiment the volunteers received 15 stimuli of each of the four conditions. Stimuli followed each other in a pseudorandomized order thus ensuring that no two adjacent stimuli were of the same kind. During each trial participants were not told which stimulus was to come. Prior to each stimulus a reaction task was performed to keep the subjects attentive: they were instructed to press a button on a button box when a white cross turned red. Following 8–10 s after each stimulus presentation, participants were asked to rate the intensity of stimuli on a visual analogue scale from 0 to 100, as well as the pleasantness of each stimulus (−50: very pleasant, 0: neutral, +50: very unpleasant). The stimulus interval was around 40 s but depended on the time consumption of the individual ratings. For a detailed description of the experiment see Kröger and May, (2015), Schulte et al. (2016), Stankewitz et al. (2013), Stankewitz and May, (2011). All participants were recruited for placebo-controlled pharmacological studies, but only data from the session on placebo control were analyzed for the current study. As a further control and to demonstrate that, although unlikely, our results are not due to a placebo effect, an independent non-placebo control group was formed from additional 18 volunteers (mean age 31.5 ± 11.1; 16 females) from another (unpublished) study following the same experimental protocol but without any association to pharmacological manipulations, and analyzed in parallel.

MR data acquisition

All magnet-resonance scanning procedures took place on a Siemens Trio 3T scanner (Siemens, Erlangen, Germany) using a 32-channel head coil. Functional data was acquired using an echo planar imaging sequence (repetition time 2.62 s, echo time 30 ms, flip angle 80°, field of view 220 mm^2, acceleration mode GRAPPA, spatial resolution 2.0×2.0×2.0 mm, acquisition matrix 110×110×40), covering the spinal trigeminal nucleus in the brainstem, cerebellum, midbrain and most of the cortex up to the face's representation in the somato-motoric homunculi. Each volume consisted of 40 axial slices (slice thickness 2 mm, gap 1 mm). After functional imaging, a high-resolution T1-weighted structural image (voxel size 1 mm^3, repetition time 2.3 s, echo time 2.98 ms, flip angle 9°, field of view 256 mm^2, 240 axial slices, slice thickness 1 mm, gap 50%) was obtained for each volunteer using a magnetization-prepared rapid gradient echo sequence.

MR data processing

Anatomical images were co-registered with the individual functional images, brainstem and cerebellum being isolated and normalized to SUIT space using the SUIT toolbox for SPM12 (Diedrichsen, 2006; Diedrichsen et al., 2009). The functional images were realigned and slice time corrected to the middle slice of each volume. Following the protocol of the SUIT toolbox the first level analyses were performed in the individual subjects' space. Only beta- and contrast images were normalized to the representative brain as defined by the SUIT space and then smoothed using a 4 mm^3 Gaussian kernel. In the first level analysis all 5 conditions (Pain, Air, Rose-odor, repetitive visual stimulation and the button press in the reaction task) were modeled by convolving a stick-function at stimulus onset with a canonical hemodynamic response function. The general linear model (GLM) further included 6 regressors for movements gathered in the previous alignment step. For the parametric analyses of the individual's intensity and unpleasantness ratings, a further mean-centered regressor modeled the parametric changes for each of the 15 painful trials. The high-pass filter was set to 128 s. For the readers' convenience all results are presented in the space provided by the Montreal Neurological Institute (MNI). Therefore the templates of the SUIT toolbox where normalized to the MNI space using the non-linear normalization routine of SPM12 (Ashburner and Friston, 2005) and the resulting deformation matrix was used to normalize the resulting peak voxel location from SUIT to MNI space.

Group analysis

To gain an insight on the areas activated during trigeminal nociception, a one-sided t-test was calculated for the contrast Ammonia-Air with second level statistics as implemented in SPM12, all masked with the cerebellar-brainstem template provided by the aforementioned SUIT toolbox for SPM restricting the analyzed volume to 30,1248 voxel (261.5 resels at an smoothness of (FWHM) 9.9×9.5×8.3 mm^3). As we expected very high effect sizes for the painful stimulation, we report our results voxel-wise family wise error (FWE) corrected at a threshold of $p < 0.05$, and reported significantly active voxels had to be part of clusters with a minimum extent of 20 voxels.

Furthermore we included the spinal trigeminal nucleus (sTN) as region of interest (ROI) within the brainstem. This region is the first relay station for incoming trigeminal pain signals. Using a sphere with 8 mm radius centered at (−4, −45, −53), a coordinate that was determined using Schulte et al. (2016), we ran a cluster-based random field theory (RFT) corrected analysis using a cluster forming threshold of $p < 0.00005$ and cluster p-value threshold of $p < 0.05$, with a minimum extent of 20 voxel. and FWE-correction ($p < 0.05$) for small volumes.

As the independent non-placebo control group was only included in the current study, to provide evidence that significant effect are not due to a placebo effect, we conducted a region of interest (ROI) analysis within this group to test for significant activations within the areas found to be activated within the main analysis (under placebo condition). Therefore we ran a cluster-based RFT corrected analysis using a cluster forming threshold of $p < 0.00005$ and cluster p-value threshold of 0.05 (FWE corrected) within a sphere of 8 mm around each of the peak voxel coordinates found to be active in the main group.

As our relative small smoothing kernel of 4 mm^3, necessary to retain the activation in the small nuclei within the brainstem, might break the smoothness assumptions of the random field theoretical approach as used in the FWE-correction of SPM12, we further replicated our findings using two non-parametric statistical methods based on 5000 permutations. First we replicated our findings using the statistic non parametric mapping (SnPM13) extension of SPM12 developed by Thomas Nichols (Nichols and Holmes, 2002) and second using the approach of threshold-free cluster enhancement (TFCE (Smith and Nichols, 2009)) also implemented as extension for SPM12 by Christian Gaser. For both methods we also choose a voxel-wise FWE-threshold at $p < 0.05$ and a minimum extent of the peak voxel's belonging cluster of 20 voxel.

To avoid breaking the results down to only peak voxel activity, and thus ignoring the remaining activation of the responding clusters, we further calculated the percentage of activation within each of the 28

predefined cerebellar regions provided by the SUIT-atlas as well as the percentage of total activation within the cerebellum in a descriptive manner. Therefore, we first calculated the total volume of each cerebellar region *i* by means of number of voxel *Vg*, which is provided by the SUIT atlas. Second, we counted the number of activated (voxel-wise FWE-corrected, $p < 0.05$) voxel *Va* in each of the regions *i*. The percentage of activated volume V*p* is then given by:

$$Vp_i = \frac{Va_i}{Vg_i} * 100.$$

The same calculation was also performed looking at the whole cerebellum as one region and thereby gaining the total activated volume of the cerebellum.

For olfactory chemosensation without nociception, i.e. the contrast Rose-Air, no voxel survived the voxel-wise FWE-correction at a threshold level of $p < 0.05$, but olfactory induced activation was present at lower thresholds ($p < 0.001$, uncorrected).

Parametric modulation

An additional analysis was performed to gain insight into the cerebellar's parametric modulation of the painful stimulation of the trigeminal nerve. Therefore, the subject's intensity and unpleasantness ratings for each trial were centered and then included into separate analyses. Results are presented for voxel passing a threshold of $p < 0.05$ (FWE-corrected) and being part of clusters with a minimum extent of 5 voxel.

As done for the main effect of the painful stimulation we used the previously described ROI analysis for the parametric modulation in the independent non-placebo control group to control for possible influence of placebo.

Functional connectivity

Functional connectivity was assessed using Psycho-Physiological-Interaction (PPI) (Friston et al., 1997) measures as implemented in SPM12, which allows detecting regional functional connectivity changes by means of higher interaction during the painful sensation. Of special interest were cerebellar-cortical as well as brainstem-cerebellar interactions. Therefore, we extracted time courses from the 6 region of interests as defined by the main results for the contrast Ammonia-Air mentioned previously within a sphere of 8 mm and used them as seed for the PPI within the aforementioned cerebellum-brainstem mask. The PPI therefore included the seed regions' time course, the interaction term, the model of the contrast Ammonia-Air (as psychological variable) and the aforementioned 6 movement regressors. Here, activations were regarded significant from a threshold of $p < 0.0005$ (uncorrected) and a minimum cluster extent of 20 voxel on.

To further gain insights into cerebellar-cortical connectivity, especially to the thalamic-cerebellar circuit, during trigeminal nociception we also calculated the PPI for the cerebellar regions within the whole acquired volume, preprocessed similar to the SUIT pipeline but using the SPM12 normalization to MNI space and an 8 mm^3 Gaussian kernel smoothing. Resulting significant voxel had to pass a voxel-wise FWE-correction at a threshold of $p < 0.05$ and be part of clusters with a minimum extent of 20 voxel. As intra-cerebellar connectivity was not hypothesized, the cerebellum was masked out for all cerebellar seed regions.

Results

Behavior

The subjects reported the ammonia as intense (mean 63.79, STD 15.05 in the main and mean 69.01, STD 19.68 in the control group on a scale from 0 to 100) and as unpleasant (mean 23.34, STD 8.29 in the main and mean 24.27, STD 20.18 in the control group on scale from −50 to 50, were −50 meant very pleasant and 50 very unpleasant), while the rose odor was rated as less intense (mean 37.50, STD 16.50 in the main and mean 34.27, STD 17.48 in the control group) and more pleasant (mean −5.28, STD 12.23 in the main and mean −3.89, STD 13.65 in the control group).

Table 1
Activations of the cerebellum and the brainstem following nociceptive, trigeminal stimulation. Coordinates are given in MNI space, while labels of the regions stem from the SUIT toolbox.

Region of the peak voxel	Cluster size (number of voxel)	MNI coordinates (x, y, z)			T-value
L VI	807	−16	−64	−26	7.80**
L VIIIa	381	−28	−52	−48	7.82**
L Crus I	75	−38	−50	−38	7.29**
Vermis VIIIa	28	−2	−66	−36	5.34**
L PAG	179	−4	−28	−10	6.74**
L sTN	20	−4	−46	−53	4.49*

L=left.
* $p < 0.05$ voxel-wise FWE-corrected (small volume).
** $p < 0.05$ voxel-wise FWE-corrected (whole volume).

Cerebellar activation

As a result of trigeminal nociceptive input the t-test revealed four significant clusters of activation within the cerebellum and a further one in the PAG (voxel-wise FWE-corrected, $p < 0.05$). The activation of the predefined region sTN became significant on cluster level and using small volume correction with a sphere of 8 mm (voxel-wise FWE-corrected, $p < 0.05$). An overview of these significant peak activations is given in Table 1 and illustrated in Fig. 1.

All of the mentioned regions where also significantly activated ($p < 0.05$, FWE-small volume corrected in a sphere of 8 mm^3 radius) in the independent non-placebo control group. The interested reader is invited to compare Fig. 1 with the results of the control group presented in the Supplementary Fig. 1, latter of course with a lower threshold for visual inspection. The negative contrast (Air-Ammonia) did not reveal any significant activation. Anatomical definitions for the cerebellar regions stem from the SUIT-atlas.

The non-parametric analyses reveal very similar results as the parametric approach. All 5 significant active peak voxel revealed by the parametric method where also found to be significantly active in both aforementioned non-parametric measures (voxel-wise FWE-corrected, $p < 0.05$, minimum cluster extent of 20 voxel). Nevertheless, the resulting number of clusters and cluster sizes slightly differ between all three statistical methods. While TFCE also revealed 5 clusters with cluster sizes up to 2520 voxel, the SnPM analysis shows 7 clusters with a maximal cluster size of 2372 voxel. The result of the non-parametric statistics are displayed in Supplementary Fig. 1.

As the location of the peak voxel but not the extent of the activated clusters only gives a limited picture of the activations in the cerebellum, we further calculated the percentage of activated volume for each of the 28 regions defined by the SUIT atlas. This analysis shows that as much as 5.37% of the cerebellum was activated. A full list of the activated regions and the percentage of volume activated is shown in Table 2. Most prominently we see activations in the left hemisphere of the cerebellum, namely in hemispheric lobules VIIIa, VI, and VIIb as well as in the Vermis (lobule VIIIa), whose volumes were activated of more than 10%. Nevertheless, activation can also be found on the right cerebellar hemisphere, contralateral to the site of stimulation. Here hemispheric lobules VI, V and lobules I-IV were activated.

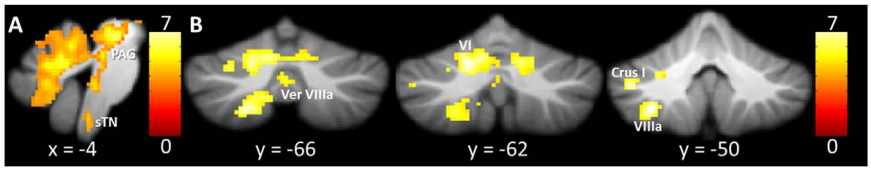

Fig. 1. Activation of the cerebellum and brainstem during nociceptive, trigeminal stimulation sketched on the MNI template. A) Brainstem activation of periaqueductal grey (PAG) and spinal trigeminal nucleus (sTN) (for visual inspection the threshold was set to $p < 0.0005$, uncorrected, cluster with minimum extent of 20 voxel). B) Cerebellar activation ($p < 0.05$, voxel-wise FWE corrected, cluster with minimum extent of 20 voxel). Coordinates are given in MNI space, while labels of the regions stem from the SUIT toolbox. The colorbar represent the T-values. Ver=Vermis.

Table 2
Regional percentage of volume activated in cerebellar areas during nociceptive, trigeminal activation.

Region	Activated Volume within the Region [%]
L VIIIa	33.5
L VI	17.7
Vermis VIIIa	13.4
L VIIb	10.3
L Crus I	7.7
L V	7.4
Vermis VI	7.1
R VI	5.3
L Crus II	4.0
R V	3.2
Vermis VIIIb	1.9
L VIIIb	1.4
L I-IV	0.6
Vermis VIIb	0.3
R I-IV	0.2
Cerebellum (overall)	5.4

L=left; R=right.

3.3. . Cerebellar activation parametrical modulated by individuals' ratings

The data shows a significant ($p < 0.05$, voxel-wise FWE-corrected) linear parametric increase of activity due to the individuals' intensity ratings in a clusters including the left hemispheric lobules V and VI of the cerebellum.

The increase of activity due to the subjects' unpleasantness ratings was present in 3 clusters, including regions VI and V as for the intensity rating and, furthermore, one cluster in the rostral part of the pons (RP). For the negative contrasts (linear decrease of activity with intensity or pleasantness ratings) no voxel survived the FWE-corrections. ROI analysis revealed significant modulation ($p < 0.05$, FWE-small volume corrected in a sphere of 8 mm^3 radius) also in the independent non-placebo control group. The activations are shown in Fig. 2 and summarized in Table 3.

Functional cerebellar-brainstem and cerebellar-cortical connectivity

Fig. 3 summarizes the aforementioned results and further sketches the increases of functional connectivity during trigeminal nociception.

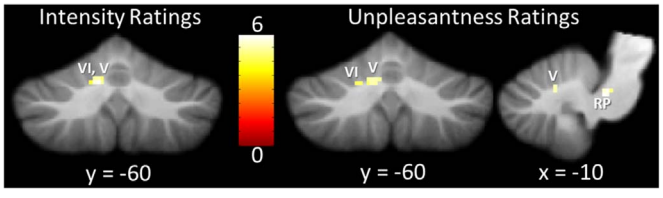

Fig. 2. Cerebellar lobules linearly increasing their activation with the subjects' intensity ratings (left hand side) or unpleasantness rating (right hand side), both with a significance level of $p < 0.05$ (voxel-wise FWE-corrected). Coordinates are given in MNI space, while labels of the regions stem from the SUIT toolbox. The colorbar represents t-values. RP=rostral Pons.

Table 3
Parametric modulations of cerebellar regions with pain intensity and unpleasantness ratings (positive correlations). Coordinates are given in MNI space, while labels of the regions stem from the SUIT toolbox.

Region	**Cluster size (number of voxel)**	**MNI coordinates of the peak voxel (x, y, z)**			**T-value**
Intensity ratings					
L VI, L V	14	−12	−62	−24	6.82**
Unpleasantness ratings					
L Periaqueductal grey (rostral Pons)	8	−10	−34	−28	6.46**
L VI, L V	11	−8	−62	−26	5.79**
L VI	5	−18	−62	−28	5.24**

L=left.
** $p < 0.05$ voxel-wise FWE-corrected (whole volume).

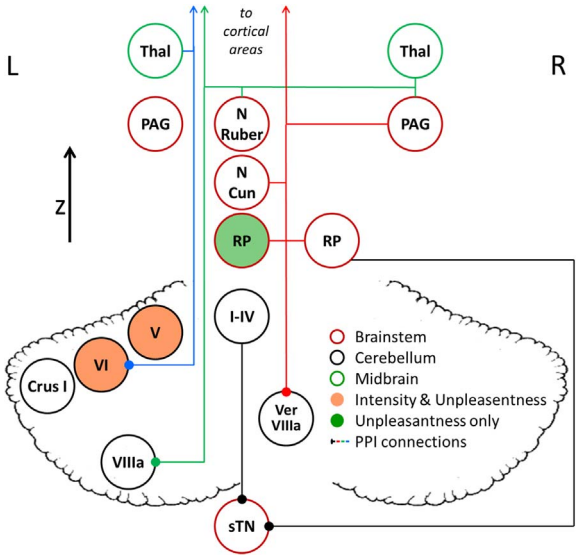

Fig. 3. Summary of cerebellar-brainstem activation, modulation and connectivity during trigeminal pain processing. Parametric modulations are represented by orange filling for the intensity and unpleasantness ratings and green for areas only modulated by the unpleasantness rating. The lines represent significant ($p < 0.05$, voxel-wise FWE-corrected) increases in interactions as achieved by physio-psychological interactions (PPI). Thal=Thalamus, PAG=periaqueductal grey, N Ruber=Nucleus Ruber, N Cun=nucleus Cuneiformis, RP=rostral Pons, I-IV=cerebellar areas I-IV, Ver=Vermis, sTN=spinal Trigeminal Nucleus.

Increased interaction of brainstem nuclei was achieved for the connections of the left spinal trigeminal nucleus with the left lobules I-VI as well as with a contralateral region within the rostral part of the pons at a threshold of $p < 0.0005$, uncorrected. A lower threshold of $p < 0.01$ (uncorrected) further revealed all cerebellar regions as found in the main analysis, except left hemispheric lobule VIIIa. The rich interaction of all three representation of the cerebellar's face areas include bilateral thalamus, contralateral PAG, red nucleus, nucleus cuneiformis and, again, rostral parts of the pons on both sides of the brainstem.

Cerebellar-cortical connectivity was significantly increased for three

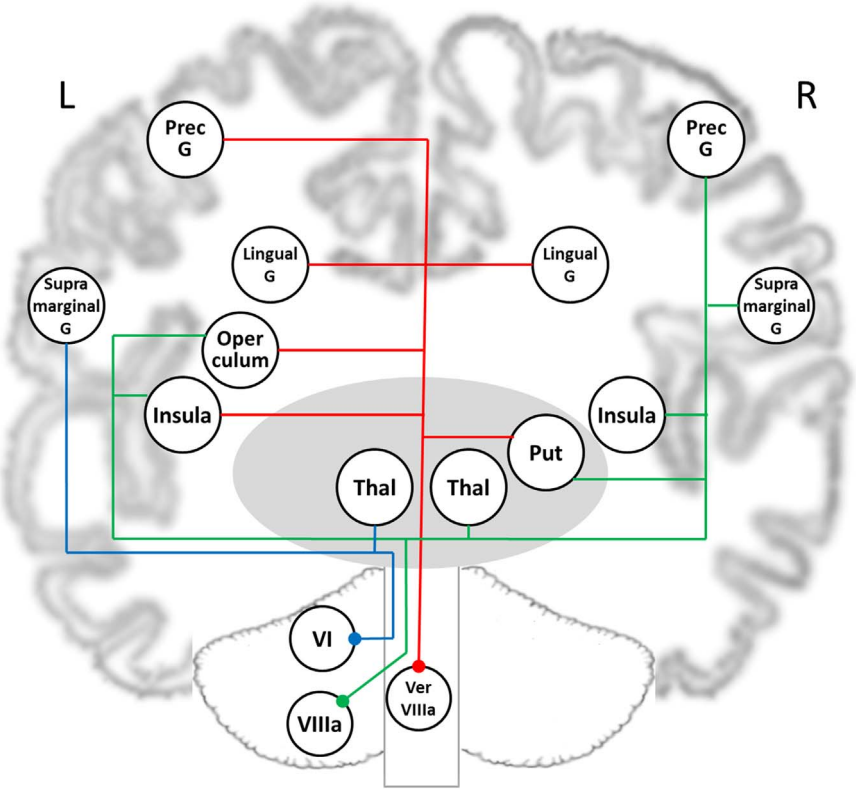

Fig. 4. Sketch of increased cerebellar-cortical interactions during trigeminal nociception resulting from the PPI analyses of three cerebellar regions, namely anterior lobule VI (blue), posterior lobule VIIIa (green), and the Vermis (lobule VIIIa, red). Prec=precentral, G=gyrus, Put=Putamen, Thal=Thalamus, Ver=Vermis.

cerebellar regions. The vermis (lobule VIIIa) showed incased interaction with the right putamen, left insula and operculum, bilateral lingual gyrus and the left precentral gyrus. The anterior left hemisphere of the cerebellum (lobule VI) increased its interaction during trigeminal pain with the ipsilateral thalamus and the left supramarginal gyrus while the posterior ipsilateral hemisphere (lobule VIIIa) shows higher functional connectivity to bilateral insula, the right putamen, left operculum as well as the right supramarginal and precentral gyrus. A schema of these interactions is sketched in Fig. 4. All PPI results of increased interactions are summarized in Table 4.

Discussion

Using a large cohort and an additional independent control group our results underline that large parts of the cerebellum are not only specifically activated in pain processing but may also play a significant role in pain perception. Trigeminal nociception is associated with a total activation of more than 5% of the total cerebellar volume in numerous lobuli, even contralateral to the stimulated side including all three representations (anterior as well as posterior hemispheres and the vermis) of the fractured homunculus. Our finding that trigeminal nociception is processed in the cerebellar anterior hemispheric lobules V and VI ipsilateral to the stimulus is in good accordance with the literature of somatic pain (Dietrichs, 1983), and extend this finding even to a linear relationship between the subject's ratings and cerebellar computing. The cerebellum is, not only in pain but probably also in headache, involved in processes which hitherto have been thought to be primarily driven by higher order cortical networks (Ruscheweyh et al., 2014). Using the identical trigeminal nociceptive experimental design, cortical areas modulated by pain intensity have already been shown (Kröger et al., 2015) while the current study shows the areas of the cerebellum involved in the perception of pain. We note that the unpleasantness ratings modulated similar areas as the intensity ratings, but involved additionally the rostral part of the pons, probably as part of the descending antinociceptive pathway.

Similar to the results of the meta-analysis by Moulton et al. (2010) our study supports the finding of a predominance of the cerebellum's hemisphere ipsilateral to the stimulation. While the vermis is associated with emotional processing (Sacchetti et al., 2009; Strata et al., 2011), the anterior hemispheric lobules have been shown to be involved in sensory and motoric processing (Stoodley and Schmahmann, 2011) whereas posterior hemispheric lobules, including Crus I and II, are mostly associated with cognitive processing such as learning (Timmann et al., 2010) and emotional processing (Moulton et al., 2011).

The increased connectivity of the spinal trigeminal nucleus with the ipsilateral lobules I-IV could be interpreted as the relay station where the mossy fibers from the sTN could terminate (Carpenter and Hanna, 1961; Huerta et al., 1983). The additional projections of the sTN to parts of the rostral pons is in good accordance with earlier findings (Kröger and May, 2015; Schulte et al., 2016). The cerebellar-brainstem interactions involve the thalamus, red nucleus and periaqueductal grey. The latter is an important hub of the descending pain processing pathway, known to modulate or even subdue pain sensation. Increased connectivity could also be shown with the nucleus cuneiformis and the rostral pons. Both regions are involved in trigeminal nociception (Schulte et al., 2016).

Next to cerebellar-brainstem networks we also found increases in cerebellar-cortical connectivity during nociception with classical regions within the “pain matrix” i.e. regions of the midbrain (thalamus), the putamen and the insula and bilateral face areas of the precentral gyrus. The role of increased connectivity between cerebellar hemispheric lobuli VI and VIIIa with bilateral supramarginal gyrus could possibly be explained by its role in processing of gustatory and chemosensation (Cerf-Ducastel et al., 2001). We note, that the aforementioned connectivity to bilateral lingual gyrus remains speculative and has also been suggested to be linked to the eye-blink reflex following trigeminal nociception (Hupé et al., 2012). However, the robust

Table 4
Increased functional cerebellar-cortical and brainstem-cerebellar connectivity. Coordinates are given in MNI space, while labels of the regions stem from the SUIT toolbox.

Region of the peak voxel (and peak voxel in sub-regions)	Cluster size (number of voxel)	MNI coordinates of the peak voxel (x, y, z)			T-value
L VI (MNI: −16, −64, −26)					
L Thalamus	29	−14	−12	2	5.35*
L Putamen	60	−28	−6	14	6.41**
L Supramarginal gyrus	21	−66	−26	20	5.74**
L VIIIa (MNI: −28, −52, −48)					
R Periaqueductal grey	25	6	−26	−4	5.37*
L Nucleus Ruber	24	−6	−24	−8	4.83*
R Thalamus	45	10	−16	−2	4.45*
L anterior Insula	310	−34	8	−14	7.09**
R Supramarginal gyrus	66	52	−36	24	6.24**
R anterior Insula	62	32	6	12	6.16**
R Precentral gyrus	223	60	−4	14	6.15**
R anterior Insula	108	38	8	−16	6.06**
L central Operculum	96	−54	0	10	5.87**
R Putamen	20	20	−8	12	5.78**
L Crus I (MNI: −38, −50, −38)					
No significant increase of interaction					
Vermis VIIIa (MNI: −2, −66, −36)					
R Periaqueductal grey (incl. B Thalamus, R Nucleus Ruber)	187	8	−30	−10	5.96*
R Periaqueductal grey (rostral Pons)	28	6	−40	−18	5.56*
L Periaqueductal grey (rostral Pons)	73	−6	−36	−18	5.28*
L Nucleus Cuneiformis	67	−12	−24	−12	4.91*
R Periaqueductal grey (rostral Pons)	24	6	−36	−28	4.76*
R Lingual gyrus	1320	2	−78	6	7.88**
L parietal Operculum	78	−50	−32	18	6.26**
L posterior Insula	114	−30	−2	−12	6.08**
L Lingual gyrus	31	−24	−58	2	5.93**
R Putamen	31	34	−2	10	5.67**
L Precentral gyrus	23	−14	−34	44	5.65**
L PAG (MNI: −4, −28, −10)					
No significant increase of interaction					
L sTN (MNI: −4, −46, −53)					
L I_IV	87	−8	−44	−16	5.65*
R Periaqueductal grey (rostral Pons)	31	8	−32	−20	4.90*

R=Right, L=left, B=Bilateral.
* Obtained within brainstem mask, 4 mm smoothing, uncorrected, $p < 0.0005$, minimum cluster extent of 20 voxel.
** Obtained from whole head, 8 mm smoothing, voxel-wise FWE-correct, $p < 0.05$, minimum cluster extent of 20 voxel.

findings of increased activity share a good overlap with the cerebellar-cortical networks in a large population analyzing functional connectivity in resting-state fMRI (Buckner et al., 2011). Given the strong link of the trigeminal system to numerous pain and headache disorders the current data might also provide a solid basis for further research on the pathological alteration of the cerebellar's activity and connectivity in primary headache and facial pain syndromes (Ellerbrock et al., 2013).

In conclusion, the current study underpins the important role of the cerebellum during trigeminal nociception with high statistical evidence using data from a large number of individuals and a further independent control group. Hereby evolves a rich picture of the cerebellum's - yet to explore - pain specific functional network to various brainstem and higher cortical areas involved in pain processing and perception.

Acknowledgment

This work was supported by the European Research Council by the 7th Framework EU-project EuroHeadPain (#602633) and by the German Research Foundation, SFB936/A5 to A.M.

Appendix A. Supporting information

Supplementary data associated with this article can be found in the online version at doi:10.1016/j.neuroimage.2017.02.023.

References

Ashburner, J., Friston, K.J., 2005. Unified segmentation. Neuroimage 26, 839–851. http://dx.doi.org/10.1016/j.neuroimage.2005.02.018.
Buckner, R.L., Krienen, F.M., Castellanos, A., Diaz, J.C., Yeo, B.T.T., 2011. The organization of the human cerebellum estimated by intrinsic functional connectivity. J. Neurophysiol. 106, 2322–2345. http://dx.doi.org/10.1152/jn.00339.2011.
Carpenter, M.B., Hanna, G.R., 1961. Fiber projections from the spinal trigeminal nucleus in the cat. J. Comp. Neurol. 117, 117–131.
Cerf-Ducastel, B., Moortele, P.-F.V., de, MacLeod, P., Bihan, D.L., Faurion, A., 2001. Interaction of gustatory and lingual somatosensory perceptions at the cortical level in the human: a functional magnetic resonance imaging study. Chem. Senses 26, 371–383. http://dx.doi.org/10.1093/chemse/26.4.371.
Diedrichsen, J., 2006. A spatially unbiased atlas template of the human cerebellum. NeuroImage 33, 127–138. http://dx.doi.org/10.1016/j.neuroimage.2006.05.056.
Diedrichsen, J., Balsters, J.H., Flavell, J., Cussans, E., Ramnani, N., 2009. A probabilistic MR atlas of the human cerebellum. NeuroImage 46, 39–46. http://dx.doi.org/10.1016/j.neuroimage.2009.01.045.
Dietrichs, E., 1983. Cerebellar cortical afferents from the periaqueductal grey in the cat. Neurosci. Lett. 41, 21–26.
Ellerbrock, I., Engel, A.K., May, A., 2013. Microstructural and network abnormalities in headache. Curr. Opin. Neurol. 26, 353–359. http://dx.doi.org/10.1097/WCO.0b013e3283633714.
Friston, K.J., Buechel, C., Fink, G.R., Morris, J., Rolls, E., Dolan, R.J., 1997. Psychophysiological and modulatory interactions in neuroimaging. NeuroImage 6, 218–229. http://dx.doi.org/10.1006/nimg.1997.0291.
Helmchen, C., Mohr, C., Erdmann, C., Petersen, D., Nitschke, M.F., 2003. Differential cerebellar activation related to perceived pain intensity during noxious thermal stimulation in humans: a functional magnetic resonance imaging study. Neurosci. Lett. 335, 202–206. http://dx.doi.org/10.1016/S0304-3940(02)01164-3.
Huerta, M.F., Frankfurter, A., Harting, J.K., 1983. Studies of the principal sensory and spinal trigeminal nuclei of the rat: projections to the superior colliculus, inferior olive, and cerebellum. J. Comp. Neurol. 220, 147–167. http://dx.doi.org/10.1002/cne.902200204.
Hupé, J.-M., Bordier, C., Dojat, M., 2012. A BOLD signature of eyeblinks in the visual cortex. NeuroImage 61, 149–161. http://dx.doi.org/10.1016/j.neuroimage.2012.03.001.
Kröger, I.L., May, A., 2015. Triptan-induced disruption of trigemino-cortical connectivity. Neurology 84, 2124–2131. http://dx.doi.org/10.1212/WNL.0000000000001610.
Kröger, I.L., Menz, M.M., May, A., 2015. Dissociating the neural mechanisms of pain consistency and pain intensity in the trigemino-nociceptive system. Cephalalgia: Int. J. headache. http://dx.doi.org/10.1177/0333102415612765.
Manni, E., Petrosini, L., 2004. A century of cerebellar somatotopy: a debated representation. Nat. Rev. Neurosci. 5, 241–249. http://dx.doi.org/10.1038/nrn1347.
May, A., 2009. New insights into headache: an update on functional and structural imaging findings. Nat. Rev. Neurol. 5, 199–209. http://dx.doi.org/10.1038/nrneurol.2009.28.
May, A., 2013. Pearls and pitfalls: neuroimaging in headache. Cephalalgia 33, 554–565. http://dx.doi.org/10.1177/0333102412467513.
Moulton, E. a, Schmahmann, J.D., Becerra, L., Borsook, D., 2010. The cerebellum and pain: passive integrator or active participator? Brain Res. Rev. 65, 14–27. http://dx.doi.org/10.1016/j.brainresrev.2010.05.005.
Moulton, E. a, Elman, I., Pendse, G., Schmahmann, J., Becerra, L., Borsook, D., 2011. Aversion-related circuitry in the cerebellum: responses to noxious heat and unpleasant images. J. Neurosci.: Off. J. Soc. Neurosci. 31, 3795–3804. http://dx.doi.org/10.1523/JNEUROSCI.6709-10.2011.
Nichols, T.E., Holmes, A.P., 2002. Nonparametric permutation tests for functional neuroimaging: a primer with examples. Human. Brain Mapp. 15, 1–25.
Rijntjes, M., Buechel, C., Kiebel, S., Weiller, C., 1999. Multiple somatotopic representations in the human cerebellum. Neuroreport 10, 3653–3658.
Ruscheweyh, R., Kühnel, M., Filippopulos, F., Blum, B., Eggert, T., Straube, A., 2014. Altered experimental pain perception after cerebellar infarction. Pain 155, 1303–1312. http://dx.doi.org/10.1016/j.pain.2014.04.006.
Saab, C.Y., Willis, W.D., 2003. The cerebellum: organization, functions and its role in nociception. Brain research. Brain Res. Rev. 42, 85–95.
Sacchetti, B., Scelfo, B., Strata, P., 2009. Cerebellum and emotional behavior. Neuroscience 162, 756–762. http://dx.doi.org/10.1016/j.neuroscience.2009.01.064.
Schulte, L.H., Sprenger, C., May, A., 2016. Physiological brainstem mechanisms of trigeminal nociception: an fMRI study at 3T. NeuroImage 124, 518–525. http://dx.doi.org/10.1016/j.neuroimage.2015.09.023.
Smith, S.M., Nichols, T.E., 2009. Threshold-free cluster enhancement: addressing problems of smoothing, threshold dependence and localisation in cluster inference. Neuroimage 44, 83–98. http://dx.doi.org/10.1016/j.neuroimage.2008.03.061.
Stankewitz, A., May, A., 2011. Increased limbic and brainstem activity during migraine attacks following olfactory stimulation. Neurology 77, 476–482. http://dx.doi.org/10.1212/WNL.0b013e318227e4a8.

Stankewitz, A., Schulz, E., May, A., 2013. Neuronal correlates of impaired habituation in response to repeated trigemino-nociceptive but not to olfactory input in migraineurs: an fMRI study. Cephalalgia: Int. J. headache 33, 256–265. http://dx.doi.org/10.1177/0333102412470215.

Stankewitz, A., Voit, H.L., Bingel, U., Peschke, C., May, A., 2010. A new trigemino-nociceptive stimulation model for event-related fMRI. Cephalalgia: Int. J. Headache 30, 475–485. http://dx.doi.org/10.1111/j.1468-2982.2009.01968.x.

Stoodley, C.J., Schmahmann, J.D., 2011. Evidence for topographic organization in the cerebellum of motor control versus cognitive and affective processing. Cortex 46, 831–844. http://dx.doi.org/10.1016/j.cortex.2009.11.008.Evidence.

Strata, P., Scelfo, B., Sacchetti, B., 2011. Involvement of cerebellum in emotional behavior. Physiol. Res. 60 (Suppl 1), S39–S48.

Timmann, D., Drepper, J., Frings, M., Maschke, M., Richter, S., Gerwig, M., Kolb, F.P., 2010. The human cerebellum contributes to motor, emotional and cognitive associative learning. A review. Cortex J. Devot. Study Nerv. Syst. Behav. 46, 845–857 . http://dx.doi.org/10.1016/j.cortex.2009.06.009.